
DIFF-BBO: DIFFUSION-BASED INVERSE MODELING FOR BLACK-BOX OPTIMIZATION

Dongxia Wu

University of California San Diego
La Jolla, CA
dowu@ucsd.edu

Nikki Lijing Kuang

University of California San Diego
La Jolla, CA
11kuang@ucsd.edu

Ruijia Niu

University of California San Diego
La Jolla, CA
rniu@ucsd.edu

Yi-An Ma

University of California San Diego
La Jolla, CA
yianma@ucsd.edu

Rose Yu

University of California San Diego
La Jolla, CA
roseyu@ucsd.edu

ABSTRACT

Black-box optimization (BBO) aims to optimize an objective function by iteratively querying a black-box oracle. This process demands sample-efficient optimization due to the high computational cost of function evaluations. While prior studies focus on forward approaches to learn surrogates for the unknown objective function, they struggle with high-dimensional inputs where valid inputs form a small subspace (e.g., valid protein sequences), which is common in real-world tasks. Recently, diffusion models have demonstrated impressive capability in learning the high-dimensional data manifold. They have shown promising performance in black-box optimization tasks but only in offline settings. In this work, we propose *diffusion-based inverse modeling for black-box optimization* (Diff-BBO), the first inverse approach leveraging diffusion models for online BBO problem. Diff-BBO distinguishes itself from forward approaches through the design of acquisition function. Instead of proposing candidates in the design space, Diff-BBO employs a novel acquisition function *Uncertainty-aware Exploration* (UaE) to propose objective function values, which leverages the uncertainty of a conditional diffusion model to generate samples in the design space. Theoretically, we prove that using UaE leads to optimal optimization outcomes. Empirically, we redesign experiments on the Design-Bench benchmark for online settings and show that Diff-BBO achieves state-of-the-art performance.

1 Introduction

Practical problems in science and engineering often involve optimizing a black-box objective function that is expensive to evaluate, such as neural network architecture design [Zoph and Le, 2016], robotics [Tesch et al., 2013], and molecular design [Sanchez-Lengeling and Aspuru-Guzik, 2018]. How to achieve a near-optimal solution while minimizing function evaluations is thus a major challenge in black-box optimization (BBO). To improve sample efficiency, sequential optimization methods iteratively generate new samples in the design space conditioning on existing data and query the black-box function for evaluation. One of the most prevailing approaches is Bayesian optimization (BO) [Kushner, 1964, Mockus, 1974]. It is a class of *forward methods* that learns a surrogate model for the objective function

with Gaussian processes (GPs), and applies an acquisition function based on the surrogate to select new data samples [Frazier, 2018].

Despite its efficacy, the curse of dimensionality limits the applicability of BO to high-dimensional problems in terms of both statistical and computational complexities [Malu et al., 2021]. Additionally, these approaches can struggle with high-dimensional inputs where valid inputs constitute a small subspace (e.g., valid protein sequences or molecular structures). Such optimization problems become exceptionally challenging, as the optimizer must navigate and avoid out-of-distribution and invalid inputs [Kumar and Levine, 2020]. Recently, a novel set of methods, termed *inverse approaches*, have been proposed to address this issue. These methods [Kumar and Levine, 2020, Krishnamoorthy et al., 2023, Kim et al., 2024] break the traditional paradigm by learning an inverse mapping from objective space back to the input space (a.k.a., the black-box function’s design domain). Leveraging state-of-the-art generative models, such as diffusion models [Song et al., 2020], these approaches effectively capture data distributions in high-dimensional input space and facilitate optimization within the data manifold [Kong et al., 2024]. Besides, diffusion models naturally provide uncertainty estimates through the probabilistic nature of the diffusion process, which can be further utilized to design informative exploration strategies to propose better candidate solutions for optimization problems. However, existing inverse methods that leverage diffusion models have only been studied in offline optimization settings, assuming access to a fixed pre-collected dataset.

In this paper, we propose Diff-BBO, an inverse approach for online black-box optimization. Diff-BBO places a distribution on the design space and represents it with a conditional diffusion model. It leverages the uncertainty of the diffusion model to query the oracle function efficiently. Compared to the existing algorithms, it enjoys scalability in solving high-dimensional Black-box Optimization (BBO) problems, sample efficiency in online settings, as well as the capability of quantifying uncertainty in inverse modeling. Our approach consists of a novel acquisition function design through the *uncertainty quantification* (UQ) of conditional diffusion model, which proposes the desired objective function values used to strategically sample the design space. We summarize our main contributions as follows:

- We present Diff-BBO, an inverse modeling approach for efficient online black-box optimization (BBO) leveraging uncertainty of conditional diffusion models.
- We provide an uncertainty decomposition into epistemic uncertainty and aleatoric uncertainty for conditional diffusion models. We rigorously analyze how uncertainty propagates throughout the denoising process of conditional diffusion model.
- We design a novel acquisition function based on the uncertainty for BBO. Theoretically, we prove that the balance between targeting higher objective values and minimizing epistemic uncertainty lead to optimal optimization outcomes.
- We demonstrate that Diff-BBO achieves state-of-the-art performance with superior sample efficiency on Design-Bench and molecular discovery task in the online BBO setting.

2 Related Work

Black-box Optimization. While recent studies aim to solve offline Black-box Optimization (BBO) using a pre-collected dataset [Li et al., 2024, Krishnamoorthy et al., 2023, Fu and Levine, 2021] without querying the oracle function, prior works in BBO have largely focused on the online setting where a model can iteratively query the function during training [Turner et al., 2021, Zhang et al., 2021, Hebbal et al., 2019, Mockus, 1974]. In online BBO, most existing algorithms belong to forward methods, including BO [Wu et al., 2023] and bandit algorithms [Agrawal and Goyal, 2012, Karbasi et al., 2023]. Forward methods build a surrogate model to approximate the black-box function and optimize sequentially. Song et al., Zhang et al. proposed Likelihood-free BO uses likelihood-free inference to extend BO to a broader class of models and utilities. It directly models the acquisition function without separately performing inference with a surrogate model. However, there is a risk where the acquisition function is over-confident. In light of the recent progress in inverse approaches [Krishnamoorthy et al., 2023, Kong et al., 2024], our work focuses on solving the online BBO by introducing a sample-efficient inverse modeling method using uncertainty-aware conditional diffusion models.

Diffusion Models. As an emerging class of generative models with strong expressiveness, diffusion models [Sohl-Dickstein et al., 2015, Song et al., 2020] have been successfully deployed across various domains including image generation [Rombach et al., 2022], reinforcement learning [Wang et al., 2022], robotics [Chi et al., 2023], etc. Notably, through the formulation of stochastic differential equations (SDEs), [Song et al., 2020] provides a unified continuous-time score-based framework for distinctive classes of diffusion models. To steer the generation towards high-quality samples of desired properties, guiding the backward data-generation process with encoded task-specific information plays an important role. Hence, different types of guidance are studied in prior works [Bansal et al., 2023, Nichol

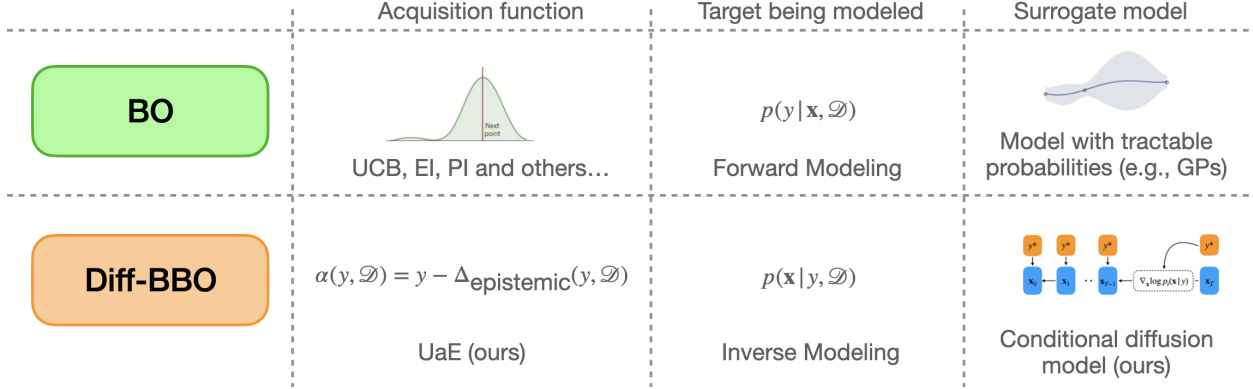


Figure 1: Forward modeling vs inverse modeling for black-box optimization. (Top) Forward modeling approach using certain surrogate models (e.g., GPs) for forward modeling and acquisition functions (e.g., UCB, PI, and EI) to select x . (Bottom) Our inverse modeling approach using generative model (e.g., diffusion model) for inverse modeling and acquisition function (e.g., UaE) to select y .

et al., 2021], including classifier guidance [Dhariwal and Nichol, 2021] where the classifier is trained externally, and classifier-free guidance [Ho and Salimans, 2022], in which the classifier is implicitly specified. In this work, we focus on classifier-free guidance to provide feasible uncertainty quantification for conditional diffusion models.

Uncertainty Quantification. Reliable uncertainty quantification (UQ) often relies on probabilistic modeling, with Bayesian approximation and ensemble learning being two popular types of approaches. Bayesian Neural Networks (BNNs) [MacKay, 1992, Neal, 2012, Kendall and Gal, 2017, Zhang et al., 2018] operate by employing variational inference (VI) to sample model weights from a tractable distribution and estimate uncertainty through sample variance. When training large-scale models, Monte Carlo (MC) dropout [Srivastava et al., 2014] offers a cost-effective alternative by approximating BNNs during inference [Gal and Ghahramani, 2016]. On the other hand, deep ensembles [Lakshminarayanan et al., 2017] train multiple NNs with different initial weights to gauge uncertainty via model variance, which also faces scalability issues as network size increases. To address this issue, recent efforts have been made to incorporate ensembling techniques with generative models to separate uncertainty into aleatoric and epistemic components [Valdenegro-Toro and Mori, 2022, Ekmekci and Cetin, 2023]. To further improve the scalability of deep ensembles, [Chan et al., 2024] proposed hyper-diffusion to quantify the uncertainty with a single diffusion model. In comparison, we take one step further by utilizing the quantified uncertainty of conditional diffusion models to solve the black-box optimization problem as a downstream task.

3 Diff-BBO

In this section, we present *Diffusion-based Inverse Modeling for Black-Box Optimization* (Diff-BBO). We first provide a probabilistic formulation of the online BBO problem along with our algorithm, followed by details of training conditional diffusion model in Diff-BBO to obtain uncertainty.

3.1 The Diff-BBO Algorithm

Let $f : \mathcal{X} \rightarrow \mathbb{R}$ denote the unknown ground-truth black-box function that evaluates the quality of any data point x , with $\mathcal{X} \subseteq \mathbb{R}^d$. Our goal is to find the optimal point x^* that maximizes f :

$$x^* \in \operatorname{argmax}_{x \in \mathcal{X}} f(x).$$

We are interested in the online BBO setting in which f is expensive to evaluate and the number of evaluations is limited. In particular, we consider batch online BBO. With a fixed query budget of Q and batch size N , we iteratively query f with N new inputs in each bath, and update the model based on observed outputs within K iterations. A key concept in online BBO is the acquisition function, which guides the selection of new query points by balancing exploration and exploitation. This function aims to efficiently identify high-performing inputs, thereby efficiently solving the online optimization problem.

In our inverse modeling approach, we model the conditional distribution of $p(x|y, \mathcal{D})$ with training data \mathcal{D} . The function value y to condition on is proposed by an acquisition function, which quantifies the quality of the generated x . The

Algorithm 1: Diff-BBO

Input: Initial dataset $\mathcal{D} = \{\mathbf{x}, y\}$, total number of iterations K , candidate feasible range C , oracle function $f(\cdot)$, batch size N

Initialization: Conditional diffusion model $p_\theta(\mathbf{x}|y)$

for $k = 1, 2, \dots, K$ **do**

- Train the conditional diffusion model with \mathcal{D}
- Construct a candidate set $\mathcal{Y} = \{y : 0 \leq y \leq C\}$
- $y_k^* = \operatorname{argmax}_{y \in \mathcal{Y}} \alpha(y, \mathcal{D})$
- Generate $\{\mathbf{x}_j\}_{j=1}^N$ where $\mathbf{x}_j \sim p_\theta(\mathbf{x} | y_k^*, \mathcal{D})$
- Query the oracle function $f(\cdot)$ with generated samples $\{\mathbf{x}_j\}_{j=1}^N$
- $\mathcal{D} \leftarrow \mathcal{D} \cup \{\mathbf{x}_j, f(\mathbf{x}_j)\}_{j=1}^N$
- $\phi_k \leftarrow \max(f(x))$ s.t. $x \in \mathcal{D}$

end

Output: Reconstructed $\{\phi_k\}_{k=1}^K$

objective of the above optimization becomes:

$$\max_{y_k \in \mathbb{R}} \sum_{k=1}^K f(\mathbf{x}_k), \quad \mathbf{x}_k \sim p_\theta(\cdot | y_k, \mathcal{D}), \quad \theta \in \Theta. \quad (1)$$

To solve the above optimization problem, we introduce Diff-BBO in Algorithm 1. At each iteration k , we train a conditional diffusion model and compute the optimal y_k^* with the designed acquisition function. In practice, y is selected from a constructed candidate set \mathcal{Y} based on the acquisition function scores $\alpha(y)$. The range of \mathcal{Y} is determined by $w \cdot \phi_k$, where w is a positive scalar and ϕ_k is the maximum function values being queried in the current training dataset \mathcal{D} . Conditioning on y_k^* , we generate N samples $\{\mathbf{x}_j\}_{j=1}^N$, where $\mathbf{x}_j \sim p_\theta(\mathbf{x} | y_k^*, \mathcal{D})$. By querying the black-box oracle to evaluate each \mathbf{x}_j , we obtain the best possible reconstructed value ϕ_k for the current iteration, and append all queried data pairs $\{\mathbf{x}_j, f(\mathbf{x}_j)\}_{j=1}^N$ to the training dataset \mathcal{D} .

Figure 1 demonstrates a detailed comparison of prior forward methods to solve the BBO problem with our proposed inverse modeling approach. Forward methods aim to learn the surrogate model $p(y|\mathbf{x}, \mathcal{D})$ for the unknown objective f by utilizing models such as GPs. However, these methods often encounter scalability issues and typically rely on heuristic approaches to generate new candidate solutions. In contrast, our approach leverages the power of diffusion model to represent $p(\mathbf{x}|y, \mathcal{D})$, allowing it to provide high-quality candidate solutions in high-dimensional problem domains and to condition on arbitrary function value. Besides, diffusion models naturally provide uncertainty estimates, which are further utilized in our design of acquisition function to solve the BBO problem.

3.2 Conditional Diffusion Model Training

Diffusion Models [Sohl-Dickstein et al., 2015, Song et al., 2020] are probabilistic generative models that learn distributions through an iterative denoising process. These models consist of three components: a forward diffusion process that produces a series of noisy samples by adding Gaussian noise, a reverse process to reconstruct the original data samples from the noise, and a sampling procedure to generate new data samples from the learned distribution. Let the original sample be \mathbf{x}_0 and t be the diffusion step. For conditional diffusion models, a conditional variable y is added to both the forward process as $q(\mathbf{x}_t | \mathbf{x}_{t-1}, y)$ and reverse process as $p_\theta(\mathbf{x}_{t-1} | \mathbf{x}_t, y), \forall t \in [T]$.

The reverse process begins with the standard Gaussian distribution $p(\mathbf{x}_T) = \mathcal{N}(\mathbf{0}, \mathbf{I})$, and denoises \mathbf{x}_t to recover \mathbf{x}_0 through the following Markov chain with reverse transitions:

$$\begin{aligned} p_\theta(\mathbf{x}_{0:T}|y) &= p(\mathbf{x}_T) \prod_{t=1}^T p_\theta(\mathbf{x}_{t-1} | \mathbf{x}_t, y), \quad \mathbf{x}_T \sim \mathcal{N}(\mathbf{0}, \mathbf{I}), \\ p_\theta(\mathbf{x}_{t-1} | \mathbf{x}_t, y) &= \mathcal{N}(\mathbf{x}_{t-1}; \mu_\theta(\mathbf{x}_t, t, y), \Sigma_\theta(\mathbf{x}_t, t, y)). \end{aligned}$$

During training, Σ_θ is empirically fixed, and μ_θ is reparametrized by a trainable denoise function $\epsilon_\theta(\mathbf{x}_t, t, y)$, which is used to estimate the noise vector ϵ that was added to input \mathbf{x}_t , and is trained by minimizing a reweighted version of the evidence lower bound (ELBO):

$$\mathcal{L}_{\text{dif}} = \mathbb{E}_{\mathbf{x}_0 \sim q(\mathbf{x}), y \sim \mathcal{N}(0, \mathbf{I}), t \sim \mathcal{U}(0, T), \mathbf{x}_t \sim q(\mathbf{x}_t | \mathbf{x}_0, y)} \left[w(t) \|\epsilon - \epsilon_\theta(\mathbf{x}_t, t, y)\|_2^2 \right]. \quad (2)$$

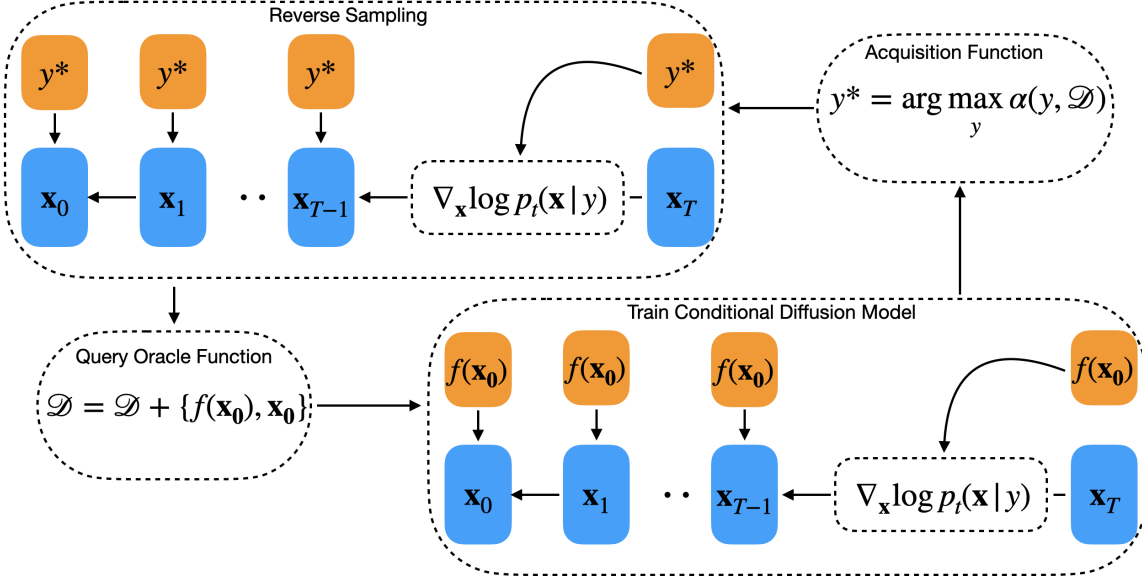


Figure 2: Black-box optimization framework using the conditional diffusion model as the inverse model. The overall framework includes 4 stages. 1. Train the conditional diffusion model given the current training dataset. 2. Compute the acquisition function and select the optimal y^* to condition on. 3. Generate samples $\{\mathbf{x}_t\}$ conditioned on y^* . 4. Query the oracle given generated samples $\{\mathbf{x}_t\}$ and update the training dataset.

Note that the loss in Equation (2) [Ho et al., 2020] for ϵ_θ is denoising score matching for all time step t , which estimates the gradient of the log probability density of the noisy data (a.k.a. score function): $\epsilon_\theta(\mathbf{x}_t, t, y) \approx -\sigma_t \nabla_{\mathbf{x}} \log p(\mathbf{x} | y)$. We further denote the score function as $s_\theta(\mathbf{x}_t, y, t) := -\epsilon_\theta(\mathbf{x}_t, t, y) / \sigma_t$.

Instead of learning a fixed deterministic θ from a deterministic neural network, we are interested in learning its Bayesian posterior to further understand and improve the model's performance as well as its reliability with uncertainty quantification. In Bayesian settings, we consider the model parameters $\theta \in \Theta$, where Θ is the parameter space, and maintain its posterior distribution $p(\theta|\mathcal{D})$, which is learned from training data \mathcal{D} . By choosing θ from its posterior, essentially we sample a score function $\tilde{s}_\theta(\mathbf{x}_t, y, t)$ from the probability distribution $p(s_\theta | \mathbf{x}_t, y, t, \mathcal{D}) = \mathcal{N}(s_\theta(\mathbf{x}_t, y, t), \Sigma_{s_\theta}(\mathbf{x}_t, y, t))$, whose expected value is $s_\theta(\mathbf{x}_t, y, t)$, and variance is a diagonal covariance matrix $\Sigma_{s_\theta}(\mathbf{x}_t, y, t)$.

Specifically, we adopt classifier-free guidance as in [Ho and Salimans, 2022] to eliminate the requirement of training a separate classifier model. We jointly train an unconditional diffusion model $p_\theta(\mathbf{x})$ parameterized by $\epsilon_\theta(\mathbf{x}, t, \emptyset)$ and a conditional diffusion model $p_\theta(\mathbf{x}|y)$ parameterized by $\epsilon_\theta(\mathbf{x}, t, y)$ by minimizing the following loss function:

$$\mathcal{L}_{\text{cdif}} = \mathbb{E}_{\mathbf{x}_0, y, \epsilon, t, \mathbf{x}_t, \lambda} \left[w(t) \|\epsilon - \epsilon_\theta(\mathbf{x}_t, t, (1 - \lambda)y + \lambda\emptyset)\|_2^2 \right], \quad (3)$$

where $\mathbf{x}_0 \sim q(\mathbf{x})$, $\epsilon \sim \mathcal{N}(0, \mathbf{I})$, $t \sim \mathcal{U}(0, T)$, $\mathbf{x}_t \sim q(\mathbf{x}_t | \mathbf{x}_0)$, $\lambda \sim \text{Bernoulli}(p_{\text{uncond}})$, and p_{uncond} is the probability of setting y to the unconditional information \emptyset . The overall Diff-BBO framework with the conditional diffusion model included is shown in Figure 2.

4 Acquisition Function Design

In this section, we analyze the uncertainty of Diff-BBO, decomposing the uncertainty into aleatoric and epistemic uncertainty. Based on the uncertainty decomposition, we propose a novel acquisition function called Uncertainty-aware Exploration (UaE). We prove that by achieving a balance between high objective values and low epistemic uncertainty, UaE effectively provides a near-optimal solution to the online BBO problem.

4.1 Uncertainty Quantification on Conditional Diffusion Model

The optimization problem defined in Equation (1) presents a probabilistic formulation of the online BBO problem using inverse modeling. Instead of searching for a single optimal point \mathbf{x} , it aims to learn a parameterized distribution $p_\theta(\mathbf{x} | y, \mathcal{D})$ for a given y , and sampling from this predictive distribution. As such, we resort to the tools of Bayesian

inference to solve this task. More specifically, given an observed value y of a sample \mathbf{x} , the objective of Bayesian inference is to estimate the predictive distribution:

$$p(\mathbf{x} | y, \mathcal{D}) = \mathbb{E}_\theta[p_\theta(\mathbf{x} | y)] = \int_\theta p_\theta(\mathbf{x} | y) p(\theta | \mathcal{D}) d\theta. \quad (4)$$

Its empirical estimation over an ensemble of M conditional diffusion models is computed as:

$$\widehat{\mathbb{E}}_\theta[p_\theta(\mathbf{x} | y)] = \frac{1}{M} \sum_{i=1}^M p_{\theta_i}(\mathbf{x} | y).$$

By Equation (4), we recognize that the uncertainty arises from two sources: uncertainty in deciding parameter θ from its posterior $p(\theta | \mathcal{D})$ and uncertainty in generating sample \mathbf{x} from a fixed diffusion model $p_\theta(\mathbf{x} | y)$ after θ is chosen. Here, let us first consider the problem of how to capture the uncertainty for a fixed diffusion model. In fact, the uncertainty in generating \mathbf{x} can be explicitly traced through the denoising process. More specifically, Theorem 1 provides analytical solutions to compute the uncertainty on a single denoising process of general score-based conditional diffusional models. It provides theoretical insights of how uncertainty is being propagated through the reverse denoising process both in discrete time and continuous time, which is characterized through the lens of stochastic differential equations (SDEs) of the Ornstein–Uhlenbeck (OU) process. Detailed proofs can be found in Appendix A.

Theorem 1. (Uncertainty propagation) *Let $t \in [T]$ be the diffusion step, $s_\theta(\mathbf{x}, y, t)$ be the score function of the corresponding diffusion model $p_\theta(\mathbf{x} | y)$. For a single conditional diffusional model $p_\theta(\mathbf{x} | y)$, the uncertainty in generating a sample \mathbf{x} can be analytically traced through the discrete-time reverse denoising process as follows:*

$$\begin{aligned} \text{Var}(\mathbf{x}_{t-1}) &= \frac{1}{4} \text{Var}(\mathbf{x}_t) + \text{Var}(s_\theta(\mathbf{x}, y, t)) + \frac{1}{2} (\mathbb{E}[\mathbf{x}_t \circ s_\theta(\mathbf{x}_t, y, t)] - \mathbb{E}[\mathbf{x}_t] \circ \mathbb{E}[s_\theta(\mathbf{x}_t, y, t)]) + I, \\ \mathbb{E}(\mathbf{x}_{t-1}) &= \frac{1}{2} \mathbb{E}(\mathbf{x}_t) + \mathbb{E}(s_\theta(\mathbf{x}, y, t)), \end{aligned}$$

where \circ is the Hadamard product, and I is the identity matrix. Similarly, in continuous-time process, the uncertainty can be captured as follows:

$$\text{Var}(\mathbf{x}_0) = (T+1)I + \text{Var} \left(\int_{t=0}^T \left(\frac{1}{2} \mathbf{x}_t + s_\theta(\mathbf{x}, y, t) \right) dt \right). \quad (5)$$

Nevertheless, performing exact Bayesian inference for uncertainty quantification when training diffusion models requires non-trivial efforts and can be computationally demanding. Hence, we introduce a practically-efficient uncertainty decomposition based on Equation (4).

4.2 Uncertainty Decomposition

To systematically analyze the effect of uncertainty in inverse modeling, we further provide a decomposition in terms of the aleatoric uncertainty and its epistemic counterpart.

The aleatoric uncertainty of the inverse problem is captured by the variance of the likelihood $p_\theta(\mathbf{x} | y)$, which is proportional to the variance of the measurement noise during sample generation, irreducible and task-inherent. To estimate the aleatoric uncertainty, we can Monte Carlo (MC) sample \mathbf{x} for N times from a learned likelihood function $p_\theta(\mathbf{x} | y)$ for fixed y, θ .

In contrast, the epistemic uncertainty is captured through the variance of the posterior distribution $p(\theta | \mathcal{D})$, which is proportional to the variance of the score network, and is reducible with the increase of training data. Recall that Θ is the parameter space that contains all possible model parameters θ , which are used to generate samples from the predictive distribution $p(\mathbf{x} | y, \mathcal{D})$. As the dataset size and quality grows, the variance of the posterior distribution shrinks, corresponding to the reduction of epistemic uncertainty in learned parameters $\theta \sim p(\theta | \mathcal{D})$.

To estimate the epistemic uncertainty, we use ensemble techniques. During the inference time, by initializing the trained ensemble models with different random seeds, we first sample M model parameters $\{\theta_i\}_{i=1}^M$ to simulate M conditional diffusion models. Then we generate N samples $\{\mathbf{x}_j\}_{j=1}^N$ for each diffusion model with corresponding parameter $\theta_i, \forall i \in [M]$. Combining the above gives a practical way to decompose and estimate the two types of uncertainty, which is formally described in Proposition 1.

Proposition 1 (Uncertainty Decomposition). *At each iteration $k \in [K]$, the overall uncertainty in inverse modeling can be decomposed into its aleatoric and epistemic components, which can be empirically measured as follows:*

$$\begin{aligned} \Delta_{\text{aleatoric}}(y, \mathcal{D}) &= \mathbb{E}_{\theta_i \sim p(\cdot | \mathcal{D})} \left[\text{Var}_{\mathbf{x}_{i,j} \sim p_{\theta_i}(\cdot | y)} (\|\mathbf{x}_{i,j}\|) \right], \quad \forall i \in [M], j \in [N]; \\ \Delta_{\text{epistemic}}(y, \mathcal{D}) &= \text{Var}_{\theta_i \sim p(\cdot | \mathcal{D})} \left(\mathbb{E}_{\mathbf{x}_{i,j} \sim p_{\theta_i}(\cdot | y)} [\|\mathbf{x}_{i,j}\|] \right), \quad \forall i \in [M], j \in [N]. \end{aligned} \quad (6)$$

4.3 Uncertainty-aware Exploration.

At each iteration $k \in [K]$ of Dif-BBO algorithm, the acquisition function proposes an optimal scalar value y_k^* as follows:

$$y_k^* = \operatorname{argmax}_y \alpha(y, \mathcal{D}),$$

which is used to generate \mathbf{x} in the design space using conditional diffusion model.

Note that to design an effective acquisition function for inverse modeling, we need to achieve a balance between high objective values y and low epistemic uncertainty. On the one hand, it is advantageous to focus on the regions in \mathcal{X} whose corresponding y is of high values. As function evaluations are expensive to perform, we prefer to generate samples \mathbf{x} conditioned on higher y , and only query the oracle for such promising samples to solve the black-box optimization task. On the other hand, we employ the epistemic uncertainty to gauge the error in the trained diffusion model. Specifically, it helps reduce the approximation error between y_k^* and the reconstructed function value $\max_{j \in [N]} f(\mathbf{x}_j)$, where $f(\cdot)$ is the black-box oracle, and $\mathbf{x}_j \sim p_\theta(\cdot | y_k^*, \mathcal{D}), \forall j \in [N]$.

We introduce the *Uncertainty-aware Exploration* (UaE) as our designed acquisition function:

$$\alpha(y, \mathcal{D}) = y - \Delta_{\text{epistemic}}(y, \mathcal{D}), \quad (7)$$

which utilizes the uncertainty estimation on conditional diffusion model as given in Proposition 1. As shown later, by balancing the exploration-exploitation trade-off, UaE provides an effective way to solve the online BBO problem.

4.4 Sub-optimality of UaE

To quantify the quality of generated samples, we theoretically analyze the sub-optimality performance gap between y_k^* and reconstructed value at each iteration. In particular, Theorem 2 and Theorem 3 demonstrate that such sub-optimality gap can be effectively handled in inverse modeling, with proofs deferred to Appendix B. We first show that by using conditional diffusion model, the expected error of the sub-optimality performance gap is zero.

Theorem 2. At each iteration $k \in [K]$, define the sub-optimality performance gap as

$$\Delta(p_\theta, y_k^*) = \left| y_k^* - \max_{j \in [N]} f(\mathbf{x}_j) \right|, \quad \text{where } \mathbf{x}_j \sim p_\theta(\cdot | y_k^*, \mathcal{D}), \quad \forall j \in [N]. \quad (8)$$

Assume that there exists some $\theta^* \sim p(\theta | \mathcal{D})$ that produces a predictive distribution $p_{\theta^*}(\cdot | \mathcal{D})$ such that it is able to generate a sample \mathbf{x}^* that perfectly reconstructs y_k^* . It can be shown that

$$\mathbb{E} [\Delta(p_\theta, y_k^*)] = 0,$$

and the empirical estimator $\hat{\mathbb{E}} [\Delta(p_\theta, y_k^*)]$ is unbiased.

Theorem 2 suggests that in expectation, the reconstructed function value $\max_{j \in [N]} f(\mathbf{x}_j)$ is able to accurately recover the provided conditional information y_k^* . Hence, in order to obtain a reasonable estimator for the optimization problem, the remaining concern goes to the variance of the gap defined in Equation (8), which is further evaluated in Theorem 3.

Theorem 3. (Sub-optimality bound) At each iteration $k \in [K]$, suppose M model parameters $\{\theta_i\}_{i=1}^M$ are generated from the ensemble model for some fixed dataset $|\mathcal{D}|$. Suppose function f is L -Lipschitz, it can be shown that the variance of the sub-optimality performance gap is equivalent to the epidemic uncertainty:

$$\operatorname{Var}_{\theta_i \sim p(\cdot | \mathcal{D})} (\Delta(p_{\theta_i}, y_k^*)) \leq cL^2 \Delta_{\text{epistemic}}(y_k^*, \mathcal{D}), \quad (9)$$

where c is some universal constant.

Theorem 3 shows that the variance of the sub-optimality performance gap can be upper bounded by the epistemic uncertainty of diffusion model. Therefore, our proposed acquisition function achieves the balance between high objective value and low epistemic uncertainty.

Finally, we prove in Theorem 4 that by adopting UaE for inverse modeling to guide the selection of generated samples for solving BBO problems, we can obtain a near-optimal solution for the optimization problem defined in Equation (1). The proof is available in Appendix C.

Theorem 4. Let \mathcal{Y} be the constructed candidate set at each iteration $k \in [K]$ in Algorithm 1. By adopting UaE as the acquisition function to guide the sample generation process in conditional diffusion model, Diff-BBO (Algorithm 1) achieves a near-optimal solution for the online BBO problem defined in Equation (1):

$$\max_{y_k \in \mathbb{R}} \sum_{k=1}^K f(\mathbf{x}_k), \quad \mathbf{x}_k \sim p_\theta(\cdot | y_k, \mathcal{D}), \quad \theta \in \Theta \Leftrightarrow \max_{y_k \in \mathcal{Y}} \sum_{k=1}^K \alpha(y_k, \mathcal{D}).$$

As a result, equipped with the novel design of UaE, Diff-BBO is a theoretically sound approach utilizing inverse modeling to effectively solve the online BBO problem.

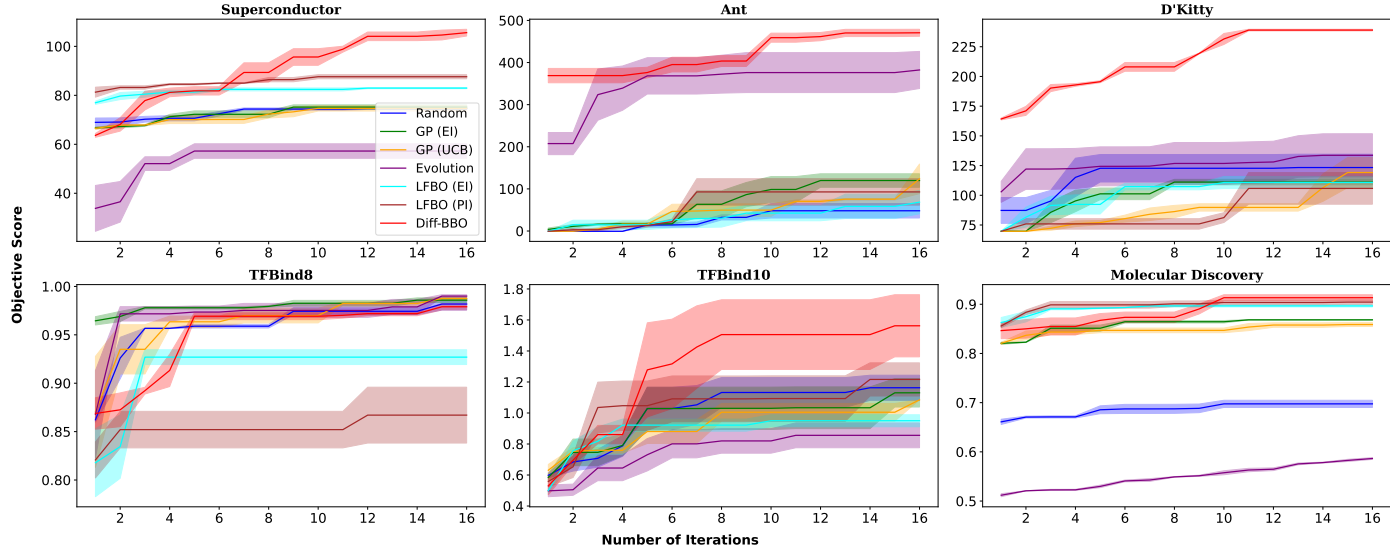


Figure 3: Comparison of Diff-BBO with baselines for online black-box optimization on DesignBench and Molecular Discovery task. We plot the mean and standard deviation across three random seeds. Diff-BBO demonstrates superior performance with very few queries to the oracle.

5 Experiments

To validate the efficacy of Diff-BBO, we conduct experiments on six real-world online black-box optimization tasks for both continuous and discrete optimization tasks. Ablation studies are performed to verify the effectiveness of the proposed acquisition function and the robustness of our model in relation to the batch size. More details of the experimental setups are provided in Appendix D.

5.1 Dataset

We restructured 5 high-dimensional real-world tasks from Design-Bench to facilitate online black-box optimization. We test on 3 continuous and 2 discrete tasks. In **D'Kitty** and **Ant** Morphology, the goal is to optimize for the morphology of robots. In **Superconductor**, the aim is to optimize for finding a superconducting material with a high critical temperature. **TFBind8** and **TFBind10** are discrete tasks where the goal is to find a DNA sequence that has a maximum affinity to bind with a specified transcription factor. We also include a **Molecular Discovery** task to optimize a compound's activity against a biological target with therapeutic value. Each optimization iteration is allocated 100 queries to the oracle function (batch size $N = 100$), with a total of 16 iterations conducted. More details of the dataset are provided in Appendix D.1.

5.2 Baselines

We consider four existing groups of baselines, including Bayesian optimization (BO), Likelihood-free BO (LFBO) [Song et al., 2022], Evolutionary algorithms [Brindle, 1980, Real et al., 2019], and random sampling. For BO approaches, we include Gaussian Processes (GP) with Monte Carlo (MC)-based batch Expected Improvement (EI) and MC-based batch Upper Confidence Bound (UCB) [Wilson et al., 2017] as the acquisition functions. For LFBO, we use EI and Probability of Improvement (PI) as the acquisition functions.

5.3 Results

Figure 3 illustrates the performance across six datasets for all baselines and our proposed algorithm. Notably, Diff-BBO consistently outperforms other baselines in both discrete and continuous settings, with the sole exception of the TFBIND-8 task. Specifically, in the Ant and Dkitty tasks, Diff-BBO demonstrates a significant lead over all baseline methods, starting from the very first iteration of the online optimization process. This remarkable performance can be attributed to Diff-BBO's diffusion model-based inverse modeling approach, which effectively learns the data manifold in the design space from the initial dataset, even when the initial dataset lacks data with high objective function values.

In contrast, the forward approach employed by BO and LFBO, which relies solely on optimizing the trained surrogate model, is more prone to converging on suboptimal solutions.

5.4 Ablation study

In this section, we conduct ablation studies to investigate the impact of our designed acquisition function, UaE. We compare Diff-BBO with the fixed condition approach. Instead of using UaE to dynamically determine which y to condition on, the fixed condition approach always generates new samples conditioned on $w \cdot \phi_k$ (Line 9 of Algorithm 1) with a fixed weight w . As shown in Figure 4, Diff-BBO consistently outperforms the fixed condition approach. This demonstrates that our acquisition function is effective in identifying the optimal y for conditioning.

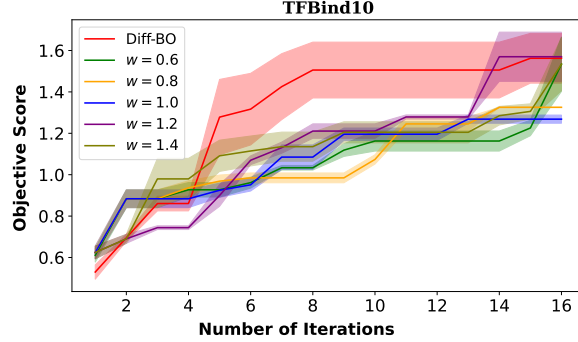


Figure 4: Impact of acquisition function design for black-box optimization on the TFBIND10 task. Comparison of Diff-BBO with five fixed-condition approaches, each with different conditioning weights. Results averaged across three random runs.

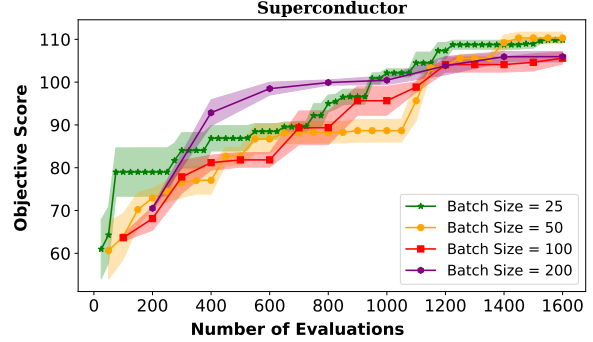


Figure 5: Ablation study to evaluate the effect of batch size on the superconductor task. The mean and standard deviation across three random seeds are plotted. Diff-BBO shows robust performances across different batch size given the same total number of evaluations.

Furthermore, we evaluate the effect of batch size, aka the number of queries per iteration on Diff-BBO on the Superconductor task. As shown in Figure 5, we compare the objective function score over number of function evaluations. We can see the performance of our approach remains similar when the batch size becomes small, suggesting remarkable robustness across different batch sizes. Hence, Diff-BBO is a highly-scalable inverse modeling approach that can efficiently leverage parallelism to handle larger computational loads without compromising performance.

6 Conclusion, Limitation, and Future Work

In this paper, we introduced Diff-BBO, a novel inverse modeling approach for black-box optimization that leverages the uncertainty of conditional diffusion models. Our method enhances the scalability in high-dimensional BBO problems and effectively quantifies uncertainty in inverse modeling. By utilizing the novel acquisition function UaE, Diff-BBO strategically proposes objective function values to improve sample efficiency in online settings. Our empirical evaluations on the Design-Bench benchmark and molecular design experiments demonstrate that Diff-BBO achieves state-of-the-art performance, establishing its potential as a robust tool for efficient and effective black-box optimization. Theoretically, we prove that using UaE leads to optimal optimization solutions.

We conclude by discussing the limitations and potential extensions of Diff-BBO: (i) *limitations with respect to diffusion modeling*: While we benefit from diffusion modeling to learn the manifold, we also inherit its drawbacks, such as slower sampling times and increased computational demands. (ii) *acquisition function improvement*: Our current implementation for the acquisition function, UaE, requires presetting the candidate sets. This necessitates additional hyperparameter tuning. (iii) *BBO extensions*: Diff-BBO can be extended to various Bayesian optimization settings, including multi-objective and multi-fidelity Bayesian optimization [Wu et al., 2023, Li et al., 2020].

Acknowledgement

This work was supported in part by the U.S. Army Research Office under Army-ECASE award W911NF-23-1-0231, the U.S. Department Of Energy, Office of Science, IARPA HAYSTAC Program, CDC-RFA-FT-23-0069, DARPA AIE FoundSci, NSF Grants #2205093, #2146343, #2134274, #2134209, and #2112665 (TILOS).

References

Barret Zoph and Quoc V Le. Neural architecture search with reinforcement learning. *arXiv preprint arXiv:1611.01578*, 2016.

Matthew Tesch, Jeff Schneider, and Howie Choset. Expensive multiobjective optimization for robotics. In *2013 ieee international conference on robotics and automation*, pages 973–980. IEEE, 2013.

Benjamin Sanchez-Lengeling and Alán Aspuru-Guzik. Inverse molecular design using machine learning: Generative models for matter engineering. *Science*, 361(6400):360–365, 2018.

Harold J Kushner. A new method of locating the maximum point of an arbitrary multipeak curve in the presence of noise. 1964.

Jonas Mockus. On bayesian methods for seeking the extremum. In *Proceedings of the IFIP Technical Conference*, pages 400–404, 1974.

Peter I Frazier. A tutorial on bayesian optimization. *arXiv preprint arXiv:1807.02811*, 2018.

Mohit Malu, Gautam Dasarathy, and Andreas Spanias. Bayesian optimization in high-dimensional spaces: A brief survey. In *2021 12th International Conference on Information, Intelligence, Systems & Applications (IISA)*, pages 1–8. IEEE, 2021.

Aviral Kumar and Sergey Levine. Model inversion networks for model-based optimization. *Advances in neural information processing systems*, 33:5126–5137, 2020.

Siddarth Krishnamoorthy, Satvik Mehul Mashkaria, and Aditya Grover. Diffusion models for black-box optimization. In *International Conference on Machine Learning*, pages 17842–17857. PMLR, 2023.

Minsu Kim, Federico Berto, Sungsoo Ahn, and Jinkyoo Park. Bootstrapped training of score-conditioned generator for offline design of biological sequences. *Advances in Neural Information Processing Systems*, 36, 2024.

Yang Song, Jascha Sohl-Dickstein, Diederik P Kingma, Abhishek Kumar, Stefano Ermon, and Ben Poole. Score-based generative modeling through stochastic differential equations. *arXiv preprint arXiv:2011.13456*, 2020.

Lingkai Kong, Yuanqi Du, Wenhao Mu, Kirill Neklyudov, Valentin De Bortol, Haorui Wang, Dongxia Wu, Aaron Ferber, Yi-An Ma, Carla P Gomes, et al. Diffusion models as constrained samplers for optimization with unknown constraints. *arXiv preprint arXiv:2402.18012*, 2024.

Zihao Li, Hui Yuan, Kaixuan Huang, Chengzhuo Ni, Yinyu Ye, Minshuo Chen, and Mengdi Wang. Diffusion model for data-driven black-box optimization. *arXiv preprint arXiv:2403.13219*, 2024.

Justin Fu and Sergey Levine. Offline model-based optimization via normalized maximum likelihood estimation. *arXiv preprint arXiv:2102.07970*, 2021.

Ryan Turner, David Eriksson, Michael McCourt, Juha Kiili, Eero Laaksonen, Zhen Xu, and Isabelle Guyon. Bayesian optimization is superior to random search for machine learning hyperparameter tuning: Analysis of the black-box optimization challenge 2020. In *NeurIPS 2020 Competition and Demonstration Track*, pages 3–26. PMLR, 2021.

Dinghuai Zhang, Jie Fu, Yoshua Bengio, and Aaron Courville. Unifying likelihood-free inference with black-box optimization and beyond. *arXiv preprint arXiv:2110.03372*, 2021.

Ali Hebbal, Loic Brevault, Mathieu Balesdent, El-Ghazali Talbi, and Nouredine Melab. Bayesian optimization using deep gaussian processes. *arXiv preprint arXiv:1905.03350*, 2019.

Dongxia Wu, Ruijia Niu, Matteo Chinazzi, Yian Ma, and Rose Yu. Disentangled multi-fidelity deep bayesian active learning. In *International Conference on Machine Learning*, pages 37624–37634. PMLR, 2023.

Shipra Agrawal and Navin Goyal. Analysis of thompson sampling for the multi-armed bandit problem. In *Conference on learning theory*, pages 39–1. JMLR Workshop and Conference Proceedings, 2012.

Amin Karbasi, Nikki Lijing Kuang, Yian Ma, and Siddharth Mitra. Langevin thompson sampling with logarithmic communication: bandits and reinforcement learning. In *International Conference on Machine Learning*, pages 15828–15860. PMLR, 2023.

Jiaming Song, Lantao Yu, Willie Neiswanger, and Stefano Ermon. A general recipe for likelihood-free bayesian optimization. In *International Conference on Machine Learning*, pages 20384–20404. PMLR, 2022.

Jascha Sohl-Dickstein, Eric Weiss, Niru Maheswaranathan, and Surya Ganguli. Deep unsupervised learning using nonequilibrium thermodynamics. In *International conference on machine learning*, pages 2256–2265. PMLR, 2015.

Robin Rombach, Andreas Blattmann, Dominik Lorenz, Patrick Esser, and Björn Ommer. High-resolution image synthesis with latent diffusion models. In *Proceedings of the IEEE/CVF conference on computer vision and pattern recognition*, pages 10684–10695, 2022.

Zhendong Wang, Jonathan J Hunt, and Mingyuan Zhou. Diffusion policies as an expressive policy class for offline reinforcement learning. *arXiv preprint arXiv:2208.06193*, 2022.

Cheng Chi, Siyuan Feng, Yilun Du, Zhenjia Xu, Eric Cousineau, Benjamin Burchfiel, and Shuran Song. Diffusion policy: Visuomotor policy learning via action diffusion. *arXiv preprint arXiv:2303.04137*, 2023.

Arpit Bansal, Hong-Min Chu, Avi Schwarzschild, Soumyadip Sengupta, Micah Goldblum, Jonas Geiping, and Tom Goldstein. Universal guidance for diffusion models. In *Proceedings of the IEEE/CVF Conference on Computer Vision and Pattern Recognition*, pages 843–852, 2023.

Alex Nichol, Prafulla Dhariwal, Aditya Ramesh, Pranav Shyam, Pamela Mishkin, Bob McGrew, Ilya Sutskever, and Mark Chen. Glide: Towards photorealistic image generation and editing with text-guided diffusion models. *arXiv preprint arXiv:2112.10741*, 2021.

Prafulla Dhariwal and Alexander Nichol. Diffusion models beat gans on image synthesis. *Advances in neural information processing systems*, 34:8780–8794, 2021.

Jonathan Ho and Tim Salimans. Classifier-free diffusion guidance. *arXiv preprint arXiv:2207.12598*, 2022.

David JC MacKay. A practical bayesian framework for backpropagation networks. *Neural computation*, 4(3):448–472, 1992.

Radford M Neal. *Bayesian learning for neural networks*, volume 118. Springer Science & Business Media, 2012.

Alex Kendall and Yarin Gal. What uncertainties do we need in bayesian deep learning for computer vision? *Advances in neural information processing systems*, 30, 2017.

Cheng Zhang, Judith Bütépage, Hedvig Kjellström, and Stephan Mandt. Advances in variational inference. *IEEE transactions on pattern analysis and machine intelligence*, 41(8):2008–2026, 2018.

Nitish Srivastava, Geoffrey Hinton, Alex Krizhevsky, Ilya Sutskever, and Ruslan Salakhutdinov. Dropout: a simple way to prevent neural networks from overfitting. *The journal of machine learning research*, 15(1):1929–1958, 2014.

Yarin Gal and Zoubin Ghahramani. Dropout as a bayesian approximation: Representing model uncertainty in deep learning. In *international conference on machine learning*, pages 1050–1059. PMLR, 2016.

Balaji Lakshminarayanan, Alexander Pritzel, and Charles Blundell. Simple and scalable predictive uncertainty estimation using deep ensembles. *Advances in neural information processing systems*, 30, 2017.

Matias Valdenegro-Toro and Daniel Saromo Mori. A deeper look into aleatoric and epistemic uncertainty disentanglement. In *2022 IEEE/CVF Conference on Computer Vision and Pattern Recognition Workshops (CVPRW)*, pages 1508–1516. IEEE, 2022.

Canberk Ekmekci and Mujdat Cetin. Quantifying generative model uncertainty in posterior sampling methods for computational imaging. In *NeurIPS 2023 Workshop on Deep Learning and Inverse Problems*, 2023.

Matthew A Chan, Maria J Molina, and Christopher A Metzler. Hyper-diffusion: Estimating epistemic and aleatoric uncertainty with a single model. *arXiv preprint arXiv:2402.03478*, 2024.

Jonathan Ho, Ajay Jain, and Pieter Abbeel. Denoising diffusion probabilistic models. *Advances in neural information processing systems*, 33:6840–6851, 2020.

Anne Brindle. Genetic algorithms for function optimization. 1980.

Esteban Real, Alok Aggarwal, Yanping Huang, and Quoc V Le. Regularized evolution for image classifier architecture search. In *Proceedings of the aaai conference on artificial intelligence*, volume 33, pages 4780–4789, 2019.

James T Wilson, Riccardo Moriconi, Frank Hutter, and Marc Peter Deisenroth. The reparameterization trick for acquisition functions. *arXiv preprint arXiv:1712.00424*, 2017.

Shibo Li, Wei Xing, Robert Kirby, and Shandian Zhe. Multi-fidelity bayesian optimization via deep neural networks. *Advances in Neural Information Processing Systems*, 33:8521–8531, 2020.

Brandon Trabucco, Xinyang Geng, Aviral Kumar, and Sergey Levine. Design-bench: Benchmarks for data-driven offline model-based optimization. In *International Conference on Machine Learning*, pages 21658–21676. PMLR, 2022.

Emanuel Todorov, Tom Erez, and Yuval Tassa. Mujoco: A physics engine for model-based control. In *2012 IEEE/RSJ international conference on intelligent robots and systems*, pages 5026–5033. IEEE, 2012.

Peter Eckmann, Kunyang Sun, Bo Zhao, Mudong Feng, Michael K Gilson, and Rose Yu. Limo: Latent inceptionism for targeted molecule generation. *arXiv preprint arXiv:2206.09010*, 2022.

Woosung Jeon and Dongsup Kim. Autonomous molecule generation using reinforcement learning and docking to develop potential novel inhibitors. *Scientific reports*, 10(1):22104, 2020.

Seul Lee, Jaehyeong Jo, and Sung Ju Hwang. Exploring chemical space with score-based out-of-distribution generation. In *International Conference on Machine Learning*, pages 18872–18892. PMLR, 2023.

Juhwan Noh, Dae-Woong Jeong, Kiyoung Kim, Sehui Han, Moontae Lee, Honglak Lee, and Yousung Jung. Path-aware and structure-preserving generation of synthetically accessible molecules. In *International Conference on Machine Learning*, pages 16952–16968. PMLR, 2022.

Garrett M Morris, Ruth Huey, William Lindstrom, Michel F Sanner, Richard K Belew, David S Goodsell, and Arthur J Olson. Autodock4 and autodocktools4: Automated docking with selective receptor flexibility. *Journal of computational chemistry*, 30(16):2785–2791, 2009.

Appendices

A Uncertainty Quantification Through SDEs

A.1 Conditional Diffusion SDE

It can be shown that the conditional diffusion model can be represented by the Ornstein–Uhlenbeck (OU) process, which is a time-homogeneous continuous-time Markov process:

$$d\mathbf{x}_t = -\gamma \mathbf{x}_t dt + \sigma d\mathbf{w}_t, \quad (10)$$

where γ is the relaxation rate, σ is the strength of fluctuation, and \mathbf{w}_t is the standard Wiener process (a.k.a., Brownian motion). Both γ and σ are time-invariant. In particular, setting $\gamma = 1$ and $\sigma = \sqrt{2}$, we are able to establish that Denoising Diffusion Probabilistic Model (DDPM) is equivalent to OU process observed at discrete times. In the remaining text, we consider SDEs for general score-based diffusion models. The SDE of the forward process in conditional diffusion model can then be written as:

$$d\mathbf{x}_t = -\frac{1}{2}g(t)\mathbf{x}_t dt + \sqrt{g(t)} d\mathbf{w}_t, \quad \mathbf{x}_0 \sim q(\mathbf{x}|y) \quad (11)$$

where $g(t)$ is a nondecreasing weighting function that controls the speed of diffusion in the forward process and $g(t) > 0$. For simplicity of analysis, we fix $g(t) = 1$ for all $t \in [T]$.

The generation process of a conditional score-based diffusion model can be viewed as a particular discretization of the following reverse-time SDE:

$$d\mathbf{x}_t = \left(\frac{1}{2}\mathbf{x}_t - \nabla_{\mathbf{x}_t} \log p(\mathbf{x}_t|y) \right) dt + d\mathbf{w}_t, \quad \mathbf{x}_0 \sim p(\mathbf{x}_T|y). \quad (12)$$

In practice, the unknown ground truth conditional score $\nabla_{\mathbf{x}_t} \log p(\mathbf{x}_t|y)$ needs to be estimated with score networks. Let such estimator denoted by $s_\theta(\mathbf{x}, y, t)$, then the conditional sample generation is to simulate the following backward SDE:

$$d\mathbf{x}_t = \left(\frac{1}{2}\mathbf{x}_t - s_\theta(\mathbf{x}, y, t) \right) dt + d\mathbf{w}_t, \quad \mathbf{x}_0 \sim \mathcal{N}(\mathbf{0}, \mathbf{I}). \quad (13)$$

In Bayesian settings, we sample a score function $\tilde{s}_\theta(\mathbf{x}_t, y, t)$ from the probability distribution $p(s_\theta|\mathbf{x}_t, y, t, \mathcal{D}) = \mathcal{N}(s_\theta(\mathbf{x}_t, y, t), \Sigma_\theta(\mathbf{x}_t, y, t))$ with expected value $s_\theta(\mathbf{x}_t, y, t)$, and diagonal covariance $\Sigma_\theta(\mathbf{x}_t, y, t)$.

A.2 Estimation of Uncertainty

In this section, we quantify the uncertainty of a single conditional diffusion model in both discrete-time and continuous-time reverse process for Theorem 1.

A.2.1 Uncertainty in Discrete-time Reverse Process

We first proof the first statement of Theorem 1. We consider the Euler discretization of Equation (13), which leads to:

$$\mathbf{x}_{t-1} = \frac{1}{2}\mathbf{x}_t + s_\theta(\mathbf{x}, y, t) + \epsilon, \quad \epsilon \sim \mathcal{N}(\mathbf{0}, \mathbf{I}). \quad (14)$$

We thus have,

$$\text{Var}(\mathbf{x}_{t-1}) = \frac{1}{4}\text{Var}(\mathbf{x}_t) + \text{Var}(s_\theta(\mathbf{x}, y, t)) + \frac{1}{2}\text{Cov}(\mathbf{x}_t, s_\theta(\mathbf{x}, y, t)) + \mathbf{I}. \quad (15)$$

$$\mathbb{E}(\mathbf{x}_{t-1}) = \frac{1}{2}\mathbb{E}(\mathbf{x}_t) + \mathbb{E}(s_\theta(\mathbf{x}, y, t)). \quad (16)$$

Here $\text{Cov}(\mathbf{x}_t, s_\theta(\mathbf{x}, y, t))$ is the element-vise covariance between \mathbf{x}_t and $s_\theta(\mathbf{x}, y, t)$. Note that we only need to consider the correlation between \mathbf{x}_t and $s_\theta(\mathbf{x}, y, t)$ at the same time step. As a result, to estimate $\text{Cov}(\mathbf{x}_t, s_\theta(\mathbf{x}, y, t))$, we have,

$$\begin{aligned} \text{Cov}(\mathbf{x}_t, s_\theta(\mathbf{x}, y, t)) &= \mathbb{E} \left[(\mathbf{x}_t - \mathbb{E}[\mathbf{x}_t]) (s_\theta(\mathbf{x}, y, t) - \mathbb{E}[s_\theta(\mathbf{x}, y, t)])^\top \right] \\ &= \mathbb{E}[\mathbf{x}_t \circ s_\theta(\mathbf{x}, y, t)] - \mathbb{E}[\mathbf{x}_t] \circ \mathbb{E}[s_\theta(\mathbf{x}, y, t)] \\ &= \mathbb{E}_{\mathbf{x}_t}[\mathbf{x}_t \circ s_\theta(\mathbf{x}, y, t)] - \mathbb{E}[\mathbf{x}_t] \circ \mathbb{E}_{\mathbf{x}_t}[s_\theta(\mathbf{x}_t, y, t)] \end{aligned} \quad (17)$$

where \circ is the Hadamard product and the third equality is by tower's rule. Substituting Equation (17) back to Equation (15) completes the proof of the first part of Theorem 1.

A.2.2 Uncertainty in Continuous-time Reverse Process

We now proof the second statement of Theorem 1. To perform the uncertainty quantification for the continuous-time reverse process, we posit the following assumption.

Assumption 1. For valid $t \in [0, T]$, the generating process \mathbf{x}_t in Equation (12) is integrable and has finite second-order moments.

With Assumption 1, integrating Equation (12) with respect to t yields:

$$\mathbf{x}_0 = \mathbf{x}_T - \int_{t=0}^T \left(\frac{1}{2} \mathbf{x}_t + \nabla_{\mathbf{x}_t} \log p(\mathbf{x}_t | y) \right) dt + \int_{t=0}^T d\mathbf{w}_t. \quad (18)$$

Applying the variance operator to both sides of

$$\begin{aligned} \text{Var}(\mathbf{x}_0) &= \text{Var}(\mathbf{x}_T) + \text{Var} \left(\int_{t=0}^T \left(\frac{1}{2} \mathbf{x}_t + \nabla_{\mathbf{x}_t} \log p(\mathbf{x}_t | y) \right) dt \right) + \text{Var} \left(\int_{t=0}^T d\mathbf{w}_t \right) \\ &= I + \text{Var} \left(\int_{t=0}^T \left(\frac{1}{2} \mathbf{x}_t + \nabla_{\mathbf{x}_t} \log p(\mathbf{x}_t | y) \right) dt \right) + \mathbb{E} \left[\left(\int_{t=0}^T d\mathbf{w}_t \right)^2 \right] - \left(\mathbb{E} \left[\int_{t=0}^T d\mathbf{w}_t \right] \right)^2 \\ &= (T+1)I + \underbrace{\text{Var} \left(\int_{t=0}^T \left(\frac{1}{2} \mathbf{x}_t + \nabla_{\mathbf{x}_t} \log p(\mathbf{x}_t | y) \right) dt \right)}_{V_1}, \end{aligned} \quad (19)$$

where the last equality follows the properties of Itô Integral and rules of stochastic calculus such that $(d\mathbf{w})^2 = dt$, $\mathbb{E}[\int_{t=0}^T d\mathbf{w}_t] = 0$. Hence, to provide an uncertainty estimate for \mathbf{x}_0 , it remains to estimate the term V_1 . Recall that the true score function $\nabla_{\mathbf{x}_t} \log p(\mathbf{x}_t | y)$ is approximated by $s_\theta((\mathbf{x}_t, y, t) = -\epsilon_\theta(\mathbf{x}_t, t, y)/\sigma_t$. For ease of notation, let $s_{\theta,t} = s_\theta(\mathbf{x}_t, y, t)$ and $\tilde{s}_{\theta,t} = \tilde{s}_\theta(\mathbf{x}_t, y, t)$, which gives

$$V_1 = \int_{t=0}^T \int_{s=0}^T \left(\frac{1}{4} \text{Cov}(\mathbf{x}_s, \mathbf{x}_t) - \frac{1}{2} \text{Cov}(\mathbf{x}_s, s_{\theta,t}) - \frac{1}{2} \text{Cov}(\mathbf{x}_t, s_{\theta,s}) + \text{Cov}(s_{\theta,t}, s_{\theta,s}) \right) ds dt.$$

When $s \neq t$, score functions $s_{\theta,t}$ and $s_{\theta,s}$ are independent, and similarly, \mathbf{x}_t and $s_{\theta,s}$ are also independent. As a result, the above equation can be further simplified as

$$V_1 = \int_{t=0}^T \int_{s=0}^T \left(\frac{1}{4} \text{Cov}(\mathbf{x}_s, \mathbf{x}_t) - \frac{1}{2} \text{Cov}(\mathbf{x}_s, s_{\theta,t}) \right) ds dt - \int_{t=0}^T (\text{Cov}(\mathbf{x}_t, s_{\theta,t}) + \text{Cov}(s_{\theta,t}, s_{\theta,t})) dt.$$

Combining all the above results together completes the proof of the second statement of Theorem 1.

B Analysis of Sub-optimality for Black-box Function

At each iteration $k \in [K]$, let y_k^* be the target function value that we condition on, and p_θ be the model learned by the conditional diffusion model. We define the performance metric for active BBO problem, which is the sub-optimal performance gap between the expected value of $\mathbf{x} \sim p_\theta(\cdot | y)$ and the target function value y^* . It is formally described as follows:

$$\Delta(p_\theta, y_k^*) = \left| y_k^* - \max_{j \in [N]} f(\mathbf{x}_j) \right|, \quad \text{where } \mathbf{x}_j \sim p_\theta(\cdot | y_k^*, \mathcal{D}), \quad \forall j \in [N]. \quad (20)$$

For simplicity of analysis, we consider $N = 1$, and let the generated sample at the k -th iteration be \mathbf{x}_k in the remaining text. We remark that all proofs go through smoothly for general N with more nuanced notations, and do not affect the conclusions being drawn. To proceed with the proofs in this section, we first state the formal assumptions for the black-box function $f(\cdot)$.

Assumption 2. The scalar black-box function f is L -Lipschitz in \mathbf{x} :

$$|f(\mathbf{x}') - f(\mathbf{x})| \leq L \|\mathbf{x}' - \mathbf{x}\|, \quad \forall \mathbf{x}', \mathbf{x} \in \mathbb{R}^d.$$

Theorem 2. At each iteration $k \in [K]$, define the sub-optimality performance gap as

$$\Delta(p_\theta, y_k^*) = \left| y_k^* - \max_{j \in [N]} f(\mathbf{x}_j) \right|, \text{ where } \mathbf{x}_j \sim p_\theta(\cdot | y_k^*, \mathcal{D}), \forall j \in [N]. \quad (8)$$

Assume that there exists some $\theta^* \sim p(\theta | \mathcal{D})$ that produces a predictive distribution $p_{\theta^*}(\cdot | \mathcal{D})$ such that it is able to generate a sample \mathbf{x}^* that perfectly reconstructs y_k^* . It can be shown that

$$\mathbb{E}[\Delta(p_\theta, y_k^*)] = 0,$$

and the empirical estimator $\widehat{\mathbb{E}}[\Delta(p_\theta, y_k^*)]$ is unbiased.

Proof of Theorem 2. For y_k^* at iteration k , since we assume the existentence of $\theta^* \sim p(\theta | \mathcal{D})$, and \mathbf{x}_j is generated from $p_\theta(\cdot | y_k^*, \mathcal{D})$, where $\theta \sim p(\theta | \mathcal{D})$ is the parameter of the diffusion model at the k -th iteration, we can express $\mathbb{E}[\Delta(p_\theta, y_k^*)]$ as follows:

$$\begin{aligned} \mathbb{E}[\Delta(p_\theta, y_k^*)] &= \mathbb{E}[\mathbb{E}[|f(\mathbf{x}^*) - f(\mathbf{x}_j)| | \mathcal{D}]] \\ &= |\mathbb{E}[\mathbb{E}[f(\mathbf{x}^* | \mathcal{D})]] - \mathbb{E}[|f(\mathbf{x}_j) | \mathcal{D}]|, \end{aligned}$$

where the first equality is by tower rule, and the second inequality is due to the fact that \mathbf{x}^* and \mathbf{x} are independent. Since the black-box function f is measurable, and by the nature of Algorithm 1, the generated sample \mathbf{x} , the proposed value y_k^* , the predictive distribution $p_\theta(\cdot | y_k^*, \mathcal{D})$, the posterior distribution $p(\theta | \mathcal{D})$ are $\sigma(\mathcal{D})$ -measurable at iteration k , the only randomness in $f(\mathbf{x})$ comes from the random sampling in the algorithm. Thus conditioned on the training data \mathcal{D} ,

$$\begin{aligned} \mathbb{E}[f(\mathbf{x}_j) | \mathcal{D}] &= \mathbb{E}[f(\mathbf{x}_j) | \mathcal{D}, p(\theta, \mathcal{D})] \\ &= \int_{\mathbf{x}} \int_{\theta} f(\mathbf{x}) p_\theta(\cdot | y_k^*, \mathcal{D}) p(\theta | \mathcal{D}) d\theta d\mathbf{x} \\ &= \mathbb{E}[f(\mathbf{x}^*) | \mathcal{D}]. \end{aligned}$$

Taking expectation of both sides completes the proof. \square

Theorem 3. (Sub-optimality bound) At each iteration $k \in [K]$, suppose M model parameters $\{\theta_i\}_{i=1}^M$ are generated from the ensemble model for some fixed dataset $|\mathcal{D}|$. Suppose function f is L -Lipschitz, it can be shown that the variance of the sub-optimality performance gap is equivalent to the epidemic uncertainty:

$$\text{Var}_{\theta_i \sim p(\cdot | \mathcal{D})}(\Delta(p_{\theta_i}, y_k^*)) \leq cL^2 \Delta_{\text{epistemic}}(y_k^*, \mathcal{D}), \quad (9)$$

where c is some universal constant.

Proof of Theorem 3. At every iteration $k \in [K]$, let the proposed function value that the conditional diffusion model conditions on be y_k^* . By Theorem 2, Conditioned on y_k^* , which is $\sigma(\mathcal{D})$ -measurable, taking the variance of both sides of Equation (20) leads to,

$$\text{Var}_{\theta_i \sim p(\cdot | \mathcal{D})}(\Delta(p_\theta, y_k^*)) = \mathbb{E}\left[\left(\Delta(p_\theta, y_k^*)\right)^2\right] - (\mathbb{E}[\Delta(p_\theta, y_k^*)])^2 = \mathbb{E}\left[\left(\Delta(p_\theta, y_k^*)\right)^2\right].$$

As a result, we only need to bound the second-order moment of $\Delta(p_\theta, y_k^*)$ with the Δ_{epidemic} . Under Assumption 2,

$$\begin{aligned} \mathbb{E}\left[\left(\Delta(p_\theta, y_k^*)\right)^2\right] &= \mathbb{E}\left[\left(y_k^* - f(\mathbf{x}_j)\right)^2\right] \\ &= \mathbb{E}\left[\left(f(\mathbf{x}_k^*) - f(\mathbf{x}_k)\right)^2\right] \\ &\leq L^2 \mathbb{E}\left[\|\mathbf{x}_k^* - \mathbf{x}_k\|^2\right]. \end{aligned}$$

Since the black-box function f is measurable, and by the nature of Algorithm 1, the generated sample \mathbf{x}_k , the proposed value y_k^* , the predictive distribution $p_\theta(\cdot | y_k^*, \mathcal{D})$, the posterior distribution $p(\theta | \mathcal{D})$ are $\sigma(\mathcal{D})$ -measurable at iteration k . Thus conditioned on the training data \mathcal{D} , with a similar argument in the proof of Theorem 2, we have

$$\mathbb{E}[\mathbf{x}_k^*] = \mathbb{E}[\mathbf{x}_k].$$

As a result,

$$\text{Var}(\Delta(p_\theta, y_k^*)) \leq L^2 \text{Var}(\mathbf{x}_k^* - \mathbf{x}_k). \quad (21)$$

Finally, by linearity of expectation,

$$\begin{aligned} \text{Var}(\mathbf{x}_k^* - \mathbf{x}_k) &= \text{Var}(\mathbf{x}_k^*) + \text{Var}(\mathbf{x}_k) + (\mathbb{E}[\mathbf{x}_k^*] - \mathbb{E}[\mathbf{x}_k])^2 - (\mathbb{E}[\mathbf{x}_k^* - \mathbf{x}_k])^2 \\ &\leq \text{Var}(\mathbf{x}_k^*) + \text{Var}(\mathbf{x}_k) = 2\text{Var}(\mathbf{x}_k). \end{aligned} \quad (22)$$

By definition of $\Delta_{\text{epidemic}}(\cdot)$, combining Equation (21) and Equation (22) completes the proof. Finally, we remark that for $N \geq 1$, \mathbf{x}_k will be replaced by $\mathbb{E}[\mathbf{x}_j]$, $\forall j \in [N]$, and is also consistent with the definition of $\Delta_{\text{epidemic}}(\cdot)$. As such, the same conclusion holds for general N . \square

C Optimality of Proposed Acquisition Function

Theorem 4. Let \mathcal{Y} be the constructed candidate set at each iteration $k \in [K]$ in Algorithm 1. By adopting UaE as the acquisition function to guide the sample generation process in conditional diffusion model, Diff-BBO (Algorithm 1) achieves a near-optimal solution for the online BBO problem defined in Equation (1):

$$\max_{y_k \in \mathbb{R}} \sum_{k=1}^K f(\mathbf{x}_k), \quad \mathbf{x}_k \sim p_\theta(\cdot | y_k, \mathcal{D}), \quad \theta \in \Theta \Leftrightarrow \max_{y_k \in \mathcal{Y}} \sum_{k=1}^K \alpha(y_k, \mathcal{D}).$$

Proof of Theorem 4. Following Theorem 3, we can express the function evaluation as follows,

$$f(\mathbf{x}_k) = y_k - (y_k - f(\mathbf{x}_k)), \quad \forall k \in [K].$$

The overall objective of the optimization problem defined in Equation (1) can then be further decomposed as

$$\begin{aligned} & \max_{y_k \in \mathbb{R}} \sum_{k=1}^K f(\mathbf{x}_k), \quad \mathbf{x}_k \sim p_\theta(\cdot | y_k), \quad \theta \in \Theta \\ & \Leftrightarrow \max_{y_k \in \mathbb{R}} \sum_{k=1}^K y_k - (y_k - f(\mathbf{x}_k)), \quad \mathbf{x}_k \sim p_\theta(\cdot | y_k), \quad \theta \in \Theta \\ & \Leftrightarrow \max_{y_k \in \mathbb{R}} \sum_{k=1}^K y_k - \Delta(p_\theta, y_k). \end{aligned}$$

By Theorem 3, which shows $\Delta(p_\theta, y_k^*)$ can be effectively upper bounded the epidemic uncertainty, we therefore have

$$\max_{y_k \in \mathbb{R}} \sum_{k=1}^K f(\mathbf{x}_k), \quad \mathbf{x}_k \sim p_\theta(\cdot | y_k), \quad \theta \in \Theta \Leftrightarrow \max_{y_k \in \mathcal{Y}} \sum_{k=1}^K y_k - \Delta_{\text{epidemic}}(y_k, \mathcal{D})$$

Essentially, our chosen acquisition function allows Diff-BBO to maximize the lower bound of the original optimization problem. \square

D Experiment Details

D.1 Dataset Details.

DesignBench [Trabucco et al., 2022] is a benchmark for real-world black-box optimization tasks. For continuous tasks, we use Superconductor, D’Kitty Morphology and Ant Morphology benchmarks. For discrete tasks, we utilize TFBind8 and TFBind10 benchmarks. We exclude Hopper due to the domain is known to be buggy, as explained in Appendix C in [Krishnamoorthy et al., 2023]. We also exclude NAS due to the significant computational resource requirement. Additionally, we exclude the ChEMBL task because the oracle model exhibits non-trivial discrepancies when queried with the same design.

- **Superconductor (materials optimization).** This task involves searching for materials with high critical temperatures. The dataset comprises 17,014 vectors, each with 86 components that represent the number of atoms of each chemical element in the formula. The provided oracle function is a pre-trained random forest regression model.
- **D’Kitty Morphology (robot morphology optimization).** This task focuses on optimizing the parameters of a D’Kitty robot, including the size, orientation, and location of the limbs, to make it suitable for a specific navigation task. The dataset consists of 10,004 entries with a parameter dimension of 56. It utilizes MuJoCO [Todorov et al., 2012], a robot simulator, as the oracle function.
- **Ant Morphology (robot morphology optimization).** Similar to D’Kitty, this task aims to optimize the parameters of a quadruped robot to maximize its speed. It includes 10,004 data points with a parameter dimension of 60. It also uses MuJoCO as the oracle function.
- **TFBind8 (DNA sequence optimization).** This task seeks to identify the DNA sequence of length eight with the highest binding affinity to the transcription factor SIX6 REF R1. The design space comprises sequences of nucleotides represented as categorical variables. The dataset size is 32,898, with a dimension of 8. The ground truth is used as a direct oracle since the affinity for the entire design space is available.

- **TFBind10 (DNA sequence optimization).** Similar to TFBind8, this task aims to find the DNA sequence of length ten that exhibits the highest binding affinity with transcription factor SIX6 REF R1. The design space consists of all possible nucleotide sequences. The dataset size is 10,000, with a dimension of 10. The ground truth is used as a direct oracle since the affinity for the entire design space is available.

Molecular Discovery. A key problem in drug discovery is the optimization of a compound’s activity against a biological target with therapeutic value. Similar to other papers [Eckmann et al., 2022, Jeon and Kim, 2020, Lee et al., 2023, Noh et al., 2022], we attempt to optimize the score from AutoDock4 [Morris et al., 2009], which is a physics-based estimator of binding affinity. The oracle is a feed-forward model as a surrogate to AutoDock4. The surrogate model is trained until convergence on 10,000 compounds randomly sampled from the latent space (using $\mathcal{N}(0, 1)$) and their computed objective values with AutoDock4. We construct our continuous design space by fixing a random protein embedding and randomly sampling 10,000 molecular embedding of dimension 32.

For all the tasks, We sort the offline dataset based on the objective values and select data from the 25% to 50% as the initial training dataset. We use data with lower objective scores to better observe performance differences across each baseline. The overview of all the task statistics is provided in Table 1.

Task	Size	Dimensions	Task Max
TFBind8	32,898	8	1.0
TFBind10	10,000	10	2.128
D’Kitty	10,004	56	340.0
Ant	10,004	60	590.0
Superconductor	17,014	86	185.0
Molecular Discovery	10,000	32	1.0

Table 1: Data Statistics

D.2 Implementation Details.

We train our model on NVIDIA A100 GPU and report the average performance over 3 random runs along with standard deviation for each task. For discrete tasks, we follow the procedure in Krishnamoorthy et al. [2023] where we convert the d -dimensional vector to a $d \times c$ one hot vector regarding c classes. We then approximate logits by interpolating between a uniform distribution and the one hot distribution using a mixing factor of 0.6. We jointly train a conditional and unconditional model with the same model by randomly set the conditioning value to 0 with dropout probability of 0.15.

For each task, we fix the learning rate at 0.001 with batch size of 256. We use 5 ensemble models to estimate the uncertainty for our acquisition function. We set hidden dimensions to 1024 and gamma to 2. We use 10% of the available data at each iteration as validation set during training.

E Impact Statement

Optimization techniques can address various real-world problems, including drug and material design. Our method enhances sample-efficient online black-box optimization, potentially accelerating solutions in these areas. However, caution is needed to prevent misuse, such as optimizing drugs to enhance harmful side effects.